RR 264

Research Report 264

AD 689447

THE ATTENUATION AND BACKSCATTERING OF INFRARED RADIATION BY ICE FOG AND WATER FOG

Motoi Kumai
and
Jack D. Russell

April 1969

D D C
JUN 3 1969

U.S. ARMY MATERIEL COMMAND
TERRESTRIAL SCIENCES CENTER
COLD REGIONS RESEARCH & ENGINEERING LABORATORY
HANOVER, NEW HAMPSHIRE

THIS DOCUMENT HAS BEEN APPROVED FOR PUBLIC RELEASE AND SALE; ITS DISTRIBUTION IS UNLIMITED.

14

Research Report 264

THE ATTENUATION AND BACKSCATTERING OF INFRARED RADIATION BY ICE FOG AND WATER FOG

Motoi Kumai

and

Jack D. Russell

Apri i 1969

DA PROJECT 1T061101A91A

U.S. ARMY MATERIEL COMMAND
TERRESTRIAL SCIENCES CENTER
COLD REGIONS RESEARCH & ENGINEERING LABORATORY
HANOVER, NEW HAMPSHIRE

THIS DOCUMENT HAS BEEN APPROVED FOR PUBLIC RELEASE
AND SALE; ITS DISTRIBUTION IS UNLIMITED.

PREFACE

This report was prepared by Dr. Motoi Kumai, Research Physicist, Research Division, Cold Regions Research and Engineering Laboratory (CRREL), U.S. Army Terrestrial Sciences Center (USA TSC). Computer work was done by SP5 Jack D. Russell of CRREL.

The report covers the optical and physical studies of ice fog undertaken by CRREL as a FY68 ILIR project with partial support from the U.S. Army Arctic Test Center. This report was published under DA Project 1T061101A91A, *In-House Laboratory Independent Research.*

USA TSC is a research activity of the Army Materiel Command.

CONTENTS

ILLUSTRATIONS

TABLES

ABSTRACT

Ice-fog crystals consisting of many spherical particles, and some hexagonal plates and columns, were observed at ambient temperatures of about -40C in the Fairbanks, Alaska, area during mid-winter. The concentrations and the size distributions of the ice-fog crystals were measured. The attenuation and back-scattering of infrared radiation by ice-fog crystals were computed for optical wavelengths of 2.2μ, 2.7μ, 4.5μ, 5.75μ, 9.7μ and 10.9μ using the Mie theory. The minimum attenuation coefficients and backscattering functions of ice fog were found to be at 9.7μ wavelength in the observed wavelengths. Optical attenuation coefficients and volume backscattering functions of water fogs were also computed using the Mie theory. The minimum attenuation coefficients and backscattering functions of water fog were found to be at 10.9μ wavelength in the region of 2.2μ, 2.7μ, 4.5μ, 5.75μ, 9.7μ and 10.9μ. Both the attenuation coefficients and back-scattering functions of ice fog are within the same order of magnitude as water fog for equivalent fog concentrations and wavelengths.

THE ATTENUATION AND BACKSCATTERING OF INFRARED RADIATION BY ICE FOG AND WATER FOG

by

Motoi Kumai and Jack D. Russell

INTRODUCTION

By reducing visibility, ice fog hampers the normal flow of traffic during severe cold weather conditions in subarctic countries. In addition, ice fog can cause extinction of the infrared beam in an infrared guidance system. Because of this, the emphasis of CRREL's ice fog research is being placed on the effects of ice fog on infrared transmission. This report presents results of a study of attenuation and backscattering of infrared radiation by fog in Alaska.

PHYSICAL PROPERTIES OF ICE FOG

The physical properties of ice fog in the Fairbanks, Alaska, area have been studied by Thuman and Robinson (1954). The formation of ice fog and its nuclei have been studied by Kumai (1964) and Kumai and O'Brien (1965).

The optical properties of fog depend on the number concentration and size distribution of the particles, which can vary significantly during different meteorological conditions. Establishing a representative fog model is not an easy task. Determination of the collection efficiency for fog droplets with radii approaching the wavelength of near-infrared radiation is one of the problems in fog sampling.

Ice-fog crystals and ice crystals are initial stages in the formation of snow crystals. Because their sizes and optical properties are quite different, it is convenient to consider them separately. Ice crystals have well-formed hexagonal plates and columns. They are often called "diamond dust" because of the way they twinkle under a low sun or under nighttime illumination. Ice crystals form at about −25C and are 20μ to 300μ in diameter. They have much lower concentrations and do not affect visibility as adversely as ice fog does. Ice-fog crystals consist of many spherical particles, equant crystals with rudimentary faces, and some hexagonal plates and columns of $2\text{-}\mu$ to $30\text{-}\mu$ diameter formed at ambient temperatures of about −40C by spontaneous nucleation (Fig. 1).

Ice-fog distributions at air temperatures of −39C and −41C in the Fairbanks, Alaska, area are shown in Figure 2 and Figure 3. The number of particles and the mass of fog per unit volume are shown as a function of crystal diameter. Table 1 summarizes the important physical properties of each fog spectrum.

Figure 1. Ice fog crystals formed at -39C ambient temperature.

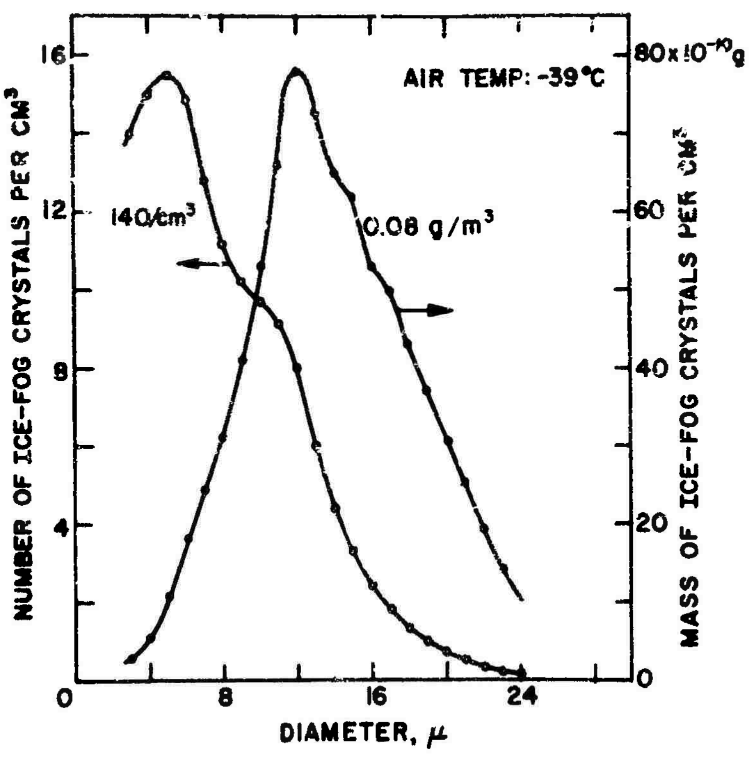

Figure 2. Size and mass distribution of ice-fog crystals formed at -39C ambient temperature.

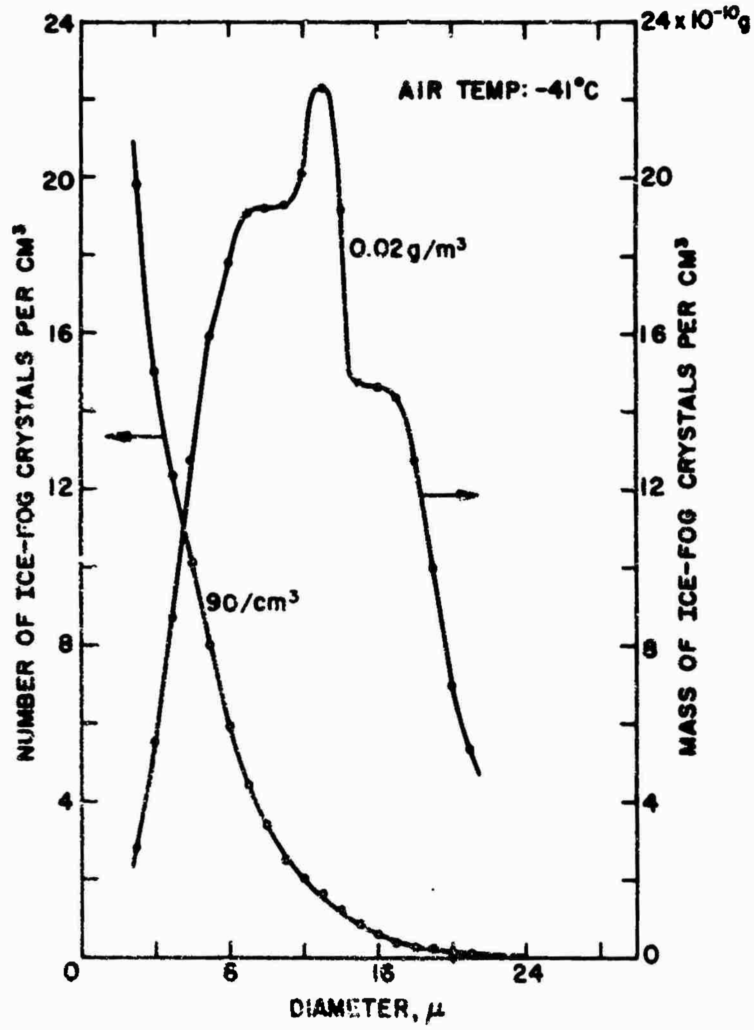

Figure 3. Size and mass distribution of ice-fog crystals formed at −41C ambient temperature.

Table I. Physical properties of ice fog at Fairbanks, Alaska.

Observations	*N* (no./cm³)	r_{mode} (μ)	r_{min} (μ)	r_{max} (μ)	Δr (μ)	*Air temp* (°C)	*L.W.C.* (g/m³)
No. 1 (Fig. 2)	140	3.0	1.5	12.0	0.5	−39	0.08
No. 2 (Fig. 3)	90	1.5	1.5	12.0	0.5	−41	0.02

N = total concentration

r_{mode} = mode radius = radius corresponding to the maximum number of ice-fog crystals

r_{min} = minimum radius

r_{max} = maximum radius

Δr = radius interval containing n(r) crystals, where $N = \sum_r n(r)$

L.W.C. = liquid water content.

MIE SCATTERING COMPUTATIONS

The Mie theory is an exact solution of Maxwell's electromagnetic theory for spheres; it describes the field inside and outside a sphere for any scattering angle, size, and index of refraction.

For backscattering, the scattering angle equals π radians. The particle size parameter is $x = k'a$ where $k' = 2\pi/\lambda$, a is the radius of the spheres, and λ is the wavelength of incident radiation.

When dealing with actual particles, scattering due to the sphere's dielectric properties alone is not sufficient to define fully the intensity of the backscattered radiation; the contribution due to absorption within the sphere must also be included. This requires a complex index of refraction of the form $m = n - ik$, where $m = (\epsilon - 4\pi i\sigma/\omega)^{1/2}$, ϵ being the dielectric constant, σ the conductivity, and ω the angular frequency of the electromagnetic wave.

The computational method as outlined in Carrier *et al.* (1967) appears quite simple at first glance. In the present study we are interested in the attenuation coefficient due to scattering, *b*, and the volume backscattering function, $\beta(\pi)$. The quantity *b* is the coefficient in the relationship

$$I = I_0 \exp(-b\ell) \tag{1}$$

defining the decrease in light intensity while passing through a medium of length ℓ.

According to the above-mentioned paper,

$$b = \sum_{r_{min}}^{r_{max}} n(r)\,\delta r\, \pi r^2 K_{ext}(x,m) \quad [\text{meter}^{-1}] \tag{2}$$

and

$$\beta(\pi) = \frac{\lambda^2}{4\pi^2} \sum_{r_{min}}^{r_{max}} n(r)\delta r i_1\,(\pi, x, m) \tag{3}$$

where $n(r)$ is the number of particles per unit volume per δr radius interval, K_{ext} is the total extinction cross section of one particle, and i_1 is the Mie intensity function of a scattered component whose electric vector is either perpendicular or parallel to the plane of observation. When $\theta = \pi$, then $i_1 = i_2$.

The problem becomes more difficult, however, when we examine the work by Deirmendjian and Clasen (1962), which outlines a computational scheme to derive values for K_{ext} and i_1. The method involves the use of ordinary Bessel functions, and circular and hyperbolic functions with complex argument. Although the functions may be reduced to fairly simple recursion formulas, the presence of complex quantities in the denominator of most of the terms requires long and tedious algebraic manipulation to make the problem programmable. It must also be kept in mind that a computer deals with pure numbers and that the real and the imaginary parts of a complex number must be dealt with individually.

The greatest consumer of computer real-time is the evaluation of the recursion formulas which consist of very slowly converging infinite series. It is not unusual to find that 300-350 terms are required to solve for just one value of the quantities K_{ext} and i_1 of which there are as many values as there are radius intervals. We must then multiply the number of radius intervals by the number of wavelengths in question when estimating total run-time.

In Figures 2 and 3, the radius interval, Δr, is 0.5μ. Particle concentrations for each fog radius $n(r_k)$ were punched on paper tape for subsequent entry into the computer. Computer calculations of the attenuation coefficient and backscattering functions from eq 2 and 3 were made for the fog size distributions of Figure 2 and Figure 3, using the optical constants of ice by Kislovskii (1959) and the optical constants of water by Centeno (1941).

The recent investigations on the optical properties of ice were done by Hornig *et al.* (1958), Ockman (1958), and Zander (1966). However, their papers do not present the values of the refractive index (n) and extinction coefficient (k) of ice. Due to the experimental difficulties, our present knowledge of the optical constants of ice in the infrared region is inexact compared with our knowledge of those of water. The optical constants of ice and water used for this computer calculation are presented in Table II (Centeno, 1941; Kislovskii, 1959).

Table II. Optical constants of ice and water.

	Ice		*Water*	
Wavelength in microns λ	*Extinction coefficient* k	*Refraction index* n	*Extinction coefficient* k	*Refraction index* n
2.2	0.0005	1.29	0.0005	1.293
2.7	0.03	1.19	0.0183	1.216
4.5	0.01	1.33	0.0164	1.341
5.75	0.01	1.24	0.0427	1.273
9.7	0.08	1.13	0.0579	1.230
10.9	0.20	1.12	0.0993	1.150

RESULTS

Optical attenuation coefficients and volume backscattering functions were computed for the observed Alaskan ice fogs for optical wavelengths of 2.2μ, 2.7μ, 4.5μ, 5.75μ, 9.7μ and 10.9μ using the Mie theory. The calculations were made for ice-fog crystal concentrations of 70, 140, 280 and 420/cm^3 with size distribution shown in Figure 2; and ice-fog crystal concentrations of 90, 180, 270 and 360/cm^3 with size distribution shown in Figure 3. The attenuation coefficients $b(m^{-1})$ and the backscattering functions $\beta(\pi)(m^{-1}sr^{-1})$ of ice-fog crystals are presented in Tables III and IV. The minimum attenuation coefficient and backscattering function are found to be at 9.7μ wavelength for the computed wavelength range of 2.2μ, 2.7μ, 4.5μ, 5.75μ, 9.7μ and 10.9μ. The optical wavelengths of 2.2μ, 9.7μ and 10.9μ are those corresponding to atmospheric windows. The wavelengths of 2.7μ and 4.5μ fall within the absorption bands of both water vapor and carbon dioxide, and the wavelength of 5.75μ is within the absorption band of water vapor.

When the air temperatures were above −15C, supercooled fogs were observed in the Fairbanks, Alaska, area during mid-winter. Optical attenuation coefficients and volume backscattering functions of water fogs were computed for optical wavelengths of 2.2μ, 2.7μ, 4.5μ, 5.75μ, 9.7μ and 10.9μ using the Mie theory. The calculations were done for fog-droplet concentrations of 70, 140, 280 and 420/cm^3 with size distributions shown in Figure 2, and fog-droplet concentrations of 90, 180, 270 and 360/cm^3 with size distributions shown in Figure 3. The attenuation coefficients $b(m^{-1})$ and the backscattering functions $\beta(\pi)(m^{-1}sr^{-1})$ of water fogs are presented in Tables III and IV. Both the attenuation coefficients and backscattering functions of ice fog and water fog are within the same order of magnitude for the same fog concentrations and wavelengths. The

Table III. The attenuation coefficients $b(m^{-1})$.

Size distribution	Concentration of fog droplets no./cm^3	Liquid water content g/m^3	Wavelength, μ 2.2	2.7	4.5	5.75	9.7	10.9
			Ice-fog					
Fig. 2	70	0.039	1.153×10^{-2}	1.212×10^{-2}	1.321×10^{-2}	1.304×10^{-2}	5.130×10^{-3}	6.795×10^{-3}
Fig. 2	140	0.077	2.306×10^{-2}	2.424×10^{-2}	2.642×10^{-2}	2.606×10^{-2}	1.026×10^{-2}	1.359×10^{-2}
Fig. 2	280	0.15	4.611×10^{-5}	4.848×10^{-5}	5.283×10^{-2}	5.216×10^{-2}	2.052×10^{-2}	2.717×10^{-2}
Fig. 2	420	0.23	6.917×10^{-5}	7.272×10^{-2}	7.925×10^{-2}	7.824×10^{-5}	3.078×10^{-2}	4.076×10^{-2}
Fig. 3	90	0.023	6.932×10^{-2}	6.694×10^{-3}	9.719×10^{-3}	7.939×10^{-3}	3.046×10^{-3}	4.206×10^{-3}
Fig. 3	180	0.047	1.786×10^{-2}	1.789×10^{-2}	1.944×10^{-2}	1.588×10^{-5}	6.092×10^{-3}	8.616×10^{-5}
Fig. 3	270	0.070	2.680×10^{-5}	2.606×10^{-5}	2.916×10^{-2}	2.382×10^{-2}	9.138×10^{-5}	1.292×10^{-2}
Fig. 3	360	0.093	3.573×10^{-2}	3.478×10^{-2}	3.883×10^{-2}	3.176×10^{-2}	1.218×10^{-5}	1.723×10^{-2}
			Water-fog					
Fig. 2	70	0.039	1.153×10^{-2}	1.217×10^{-2}	1.314×10^{-2}	1.282×10^{-2}	7.848×10^{-3}	5.455×10^{-3}
Fig. 2	140	0.077	2.305×10^{-2}	2.434×10^{-2}	2.628×10^{-2}	2.564×10^{-2}	1.568×10^{-2}	1.091×10^{-2}
Fig. 2	280	0.15	4.611×10^{-2}	4.868×10^{-5}	5.256×10^{-2}	5.127×10^{-2}	3.137×10^{-2}	2.182×10^{-2}
Fig. 2	420	0.23	8.916×10^{-5}	7.303×10^{-2}	7.886×10^{-2}	7.691×10^{-2}	4.705×10^{-5}	3.273×10^{-5}
Fig. 3	90	0.023	6.919×10^{-3}	9.054×10^{-3}	9.675×10^{-3}	8.256×10^{-3}	4.504×10^{-3}	3.255×10^{-3}
Fig. 3	180	0.047	1.784×10^{-2}	1.811×10^{-2}	1.935×10^{-5}	1.651×10^{-5}	9.008×10^{-3}	6.509×10^{-3}
Fig. 3	270	0.070	2.673×10^{-2}	2.716×10^{-2}	2.902×10^{-2}	2.477×10^{-2}	1.351×10^{-2}	9.764×10^{-3}
Fig. 3	360	0.093	3.566×10^{-2}	3.622×10^{-2}	3.870×10^{-2}	3.303×10^{-2}	1.802×10^{-5}	1.302×10^{-3}

Table IV. The backscattering functions $\beta(\pi)(m^{-1}sr^{-1})$.

Size distribution	Concentration of fog droplets no./cm^3	Liquid water content g/m^3	Wavelength, μ 2.2	2.7	4.5	5.75	9.7	10.9
			Ice-fog					
Fig. 2	70	0.039	4.804×10^{-4}	9.186×10^{-6}	1.251×10^{-5}	2.695×10^{-2}	2.[illegible]64$\times10^{-6}$	5.450×10^{-5}
Fig. 2	140	0.077	9.609×10^{-4}	1.827×10[illegible]	2.501×10^{-4}	5.389×10^{-2}	5.927×10^{-6}	1.090×10^{-5}
Fig. 2	280	0.15	1.922×10^{-3}	3.654×10^{-5}	5.002×10^{-4}	1.073×10^{-4}	1.185×10^{-2}	2.180×10^{-5}
Fig. 2	420	0.23	2.888×10^{-3}	5.481×10^{-5}	7.502×10^{-4}	7.502×10^{-4}	1.773×10^{-2}	3.271×10^{-2}
Fig. 3	90	0.023	2.744×10^{-4}	5.794×10^{-6}	7.515×10^{-5}	1.936×10^{-3}	2.485×10^{-6}	4.569×10^{-6}
Fig. 3	180	0.047	5.489×10^{-4}	1.159×10^{-5}	1.508×10^{-4}	3.372×10^{-5}	4.970×10^{-6}	9.179×10^{-6}
Fig. 3	270	0.070	8.238×10^{-4}	1.788×10^{-5}	2.255×10^{-4}	5.[illegible]08$\times10^{-2}$	7.455×10^{-5}	1.377×10^{-2}
Fig. 3	360	0.093	1.098×10^{-3}	2.818×10^{-5}	3.006×10^{-4}	7.745×10^{-5}	9.940×10^{-5}	1.886×10^{-5}
			Water-fog					
Fig. 2	70	0.039	[illegible]960$\times10^{-4}$	2.699×10^{-2}	9.400×10^{-3}	1.535×10^{-5}	1.170×10^{-6}	4.108×10^{-6}
Fig. 2	140	0.077	9.960×10^{-4}	5.397×10^{-5}	1.88[illegible]$\times10^{-4}$	3.070×10^{-5}	2.339×10^{-5}	3.206×10^{-6}
Fig. 2	280	0.15	1.992×10^{-5}	1.079×10^{-4}	8.760×10^{-4}	8.181×10^{-5}	4.679×10^{-5}	1.641×10^{-5}
Fig. 2	420	0.23	2.988×10^{-2}	1.819×10^{-4}	5.640×10^{-4}	9.271×10^{-5}	7.018×10^{-2}	2.462×10^{-5}
Fig. 3	90	0.023	2.873×10^{-4}	1.673×10^{-2}	5.990×10^{-2}	1.816×10^{-2}	8.983×10^{-6}	8.465×10^{-4}
Fig. 3	180	0.047	5.745×10^{-4}	3.846×10[illegible]	1.198×10^{-4}	2.632×10^{-5}	1.783×10^{-5}	6.981×10^{-6}
Fig. 3	270	0.070	8.618×10^{-4}	5.019×10^{-5}	1.796×10^{-4}	3.948×10^{-5}	2.680×10^{-5}	1.040×10^{-5}
Fig. 3	360	0.093	1.149×10^{-2}	6.892×10^{-5}	2.395×10^{-4}	5.265×10^{-2}	8.573×10^{-5}	1.386×10^{-2}

minimum attenuation coefficient and backscattering functions of water fog were found to be at 10.9μ wavelength for the observed wavelengths of 2.2μ, 2.7μ, 4.5μ, 5.75μ, 9.7μ, and 10.9μ.

These calculations describe only the effect of water droplets and ice crystals on the attenuation and scattering of radiation. For computations of total attenuation and scattering, the effects of the atmospheric absorption bands, especially water vapor and CO_2, would also have to be considered.

LITERATURE CITED

Carrier, L.W., Cato, G.A. and von Essen, K.J. (1967) The backscattering and extinction of visible and infrared radiation by selected major cloud models. *Applied Optics*, vol. 6, p. 1209.

Centeno, M. (1941) The refractive index of liquid water in the near infra-red spectrum. *Journal of the Optical Society of America*, vol. 31, p. 244.

Deirmendjian, D. and Clasen, R.J. (1962) Light scattering of partially absorbing homogeneous spheres of finite size. The Rand Corporation, Report R-393-PR.

Hornig, D.F., White, H.F. and Reding, F.P. (1958) The infrared spectra of crystalline H_2O, D_2O, and HDO. *Spectrochimica Acta.*, vol. 12, p. 338.

Kisiovskii, L.D. (1959) Optical characteristics of water and ice in the infrared and radiowave regions of the spectrum. *Optika i Spectroskopiia*, vol. 7, p. 311.

Kumai, M. (1964) A study of ice fog and ice-fog nuclei at Fairbanks, Alaska. U.S. Army Cold Regions Research and Engineering Laboratory (USA CRREL) Research Report 150, Part I.

________ and O'Brien (1965) A study of ice fog and ice-fog nuclei at Fairbanks, Alaska. USA CRREL Research Report 150, Part II.

Ockman, N. (1958) The infrared and Raman spectra of ice. *Advances in Physics*, vol. 7, p. 199.

Thuman, W.C. and Robinson, E. (1954) Studies of Alaskan ice-fog particles. *Journal of Meteorology*, vol. 16, p. 151-156.

Zander, R. (1966) Spectral scattering properties of ice clouds and hoarfrost. *Journal of Geophysical Research*, vol. 71, p. 375-378.

Unclassified
Security Classification

DOCUMENT CONTROL DATA - R & D

(Security classification of title, body of abstract and indexing annotation must be entered when the overall report is classified)

1. ORIGINATING ACTIVITY (Corporate author) Cold Regions Research and Engineering Laboratory U.S. Army Terrestrial Sciences Center, Hanover, New Hampshire 03755	2a. REPORT SECURITY CLASSIFICATION Unclassified 2b. GROUP

3. REPORT TITLE

THE ATTENUATION AND BACKSCATTERING OF INFRARED RADIATION BY ICE FOG AND WATER FOG

4. DESCRIPTIVE NOTES (Type of report and inclusive dates)

Research Report

5. AUTHOR(S) (First name, middle initial, last name)

Motoi Kumai and Jack D. Russell

6. REPORT DATE	7a. TOTAL NO. OF PAGES	7b. NO. OF REFS
April 1969	11	10

8a. CONTRACT OR GRANT NO. b. PROJECT NO. DA Project 1T061101A91A c. d.	9a. ORIGINATOR'S REPORT NUMBER(S) Research Report 264 9b. OTHER REPORT NO(S) (Any other numbers that may be assigned this report)

10. DISTRIBUTION STATEMENT

This document has been approved for public release and sale; its distribution is unlimited.

11. SUPPLEMENTARY NOTES Partial support from: U.S. Army Arctic Test Center Ft. Greely, Alaska	12. SPONSORING MILITARY ACTIVITY Cold Regions Research & Engineering Laboratory, U.S. Army Terrestrial Sciences Center, Hanover, New Hampshire 03755

13. ABSTRACT

Ice-fog crystals consisting of many spherical particles, and some hexagonal plates and columns, were observed at ambient temperatures of about -40C in the Fairbanks, Alaska, area during mid-winter. The concentrations and the size distributions of the ice-fog crystals were measured. The attenuation and backscattering of infrared radiation by ice-fog crystals were computed for optical wavelengths of 2.2μ, 2.7μ, 4.5μ, 5.75μ, 9.7μ and 10.9μ using the Mie theory. The minimum attenuation coefficients and backscattering functions of ice fog were found to be at 9.7μ wavelength in the observed wavelengths. Optical attenuation coefficients and volume backscattering functions of water fogs were also computed using the Mie theory. The minimum attenuation coefficients and backscattering functions of water fog were found to be at 10.9μ wavelength in the region of 2.2μ, 2.7μ, 4.5μ, 5.75μ, 9.7μ and 10.9μ. Both the attenuation coefficients and backscattering functions of ice fog are within the same order of magnitude as water fog for equivalent fog concentrations and wavelengths.

14. Key Words

Ice fog
Infrared
Alaska - meteorology

DD FORM 1 NOV 65 1473 REPLACES DD FORM 1473, 1 JAN 64, WHICH IS OBSOLETE FOR ARMY USE.

Unclassified
Security Classification